Supplemental material: Abrupt transition between three and two-dimensional quantum turbulence

Nicolás P. Müller[1,3], Marc-Etienne Brachet[2], Alexandros Alexakis[2], and Pablo D. Mininni[1]
[1] *Universidad de Buenos Aires, Facultad de Ciencias Exactas y Naturales, Departamento de Física, & IFIBA, CONICET, Ciudad Universitaria, Buenos Aires 1428, Argentina.*
[2] *Laboratoire de Physique de l'École Normale Supérieure, ENS, Université PSL, CNRS, Sorbonne Université, Université de Paris, F-75005 Paris, France and*
[3] *Université Côte d'Azur, Observatoire de la Côte d'Azur, CNRS, Laboratoire Lagrange, Nice, France*

THE GROSS-PITAEVSKII EQUATION

In this work we study a system of weakly interacting bosons of mass m at zero-temperature that is described by the GPE

$$i\hbar\frac{\partial\psi}{\partial t} = -\frac{\hbar^2}{2m}\nabla^2\psi + g|\psi|^2\psi, \tag{1}$$

where ψ is the wave function of the condensate and $g = \hbar c/(\sqrt{2}\rho_0\xi)$ is proportional to the scattering length (with c the speed of sound, ρ_0 the mean mass density, and ξ the healing length); in terms of these variables $m = \hbar/(\sqrt{2}c\xi)$. In dimensionless units, all simulations have $\rho_0 = 1$, $c = 2$, and ξ such that the vortex cores are well resolved by the spatial resolution considered. This results in $\xi = (40\sqrt{2})^{-1}$ in all simulations with $N_x = N_y = 256$ spatial grid points, and $\xi = (80\sqrt{2})^{-1}$ in all simulations with $N_x = N_y = 512$ grid points so that $\xi k_{max} = 1.5$ where k_{max} is the maximum resolved wavenumber.

The total energy $E_{\rm tot}$ is a conserved magnitude in the GPE, and can be decomposed into

$$E_{\rm tot} = E_k + E_{\rm int} + E_q, \tag{2}$$

where E_k is the kinetic energy, $E_{\rm int}$ is the internal energy, and E_q is the quantum energy, which are defined respectively as

$$E_k = \int \frac{(\sqrt{\rho}u)^2}{2} d^3r, \qquad E_{\rm int} = \int \frac{g\rho^2}{2m^2} d^3r, \qquad E_q = \int \frac{\hbar^2}{2m^2}(\boldsymbol{\nabla}\sqrt{\rho})^2 d^3r, \tag{3}$$

where ρ is the fluid density and $\boldsymbol{u}$ the fluid velocity, obtained from Madelung's transformation with $\rho = |\psi|^2$ and $\boldsymbol{u} = \hbar\boldsymbol{\nabla}\phi/m$. In this description, quantized vortices correspond to lines with $\rho = 0$, with quantum of circulation $\Gamma = h/m$. The Helmholtz decomposition $\sqrt{\rho}\boldsymbol{u} = (\sqrt{\rho}\boldsymbol{u})_i + (\sqrt{\rho}\boldsymbol{u})_c$ can be applied to the kinetic energy to further decompose it into incompressible E_k^i and compressible E_k^c kinetic energy components [1, 2]. As these energies are quadratic, it is straightforward to construct power spectra from them as

$$E_k^{i,c}(k) = \int \frac{1}{2}\left|\widehat{(\sqrt{\rho}u)_{i,c}}\right|^2 k^2 d\Omega_k, \qquad E_{\rm int}(k) = \int \frac{g\,|\widehat{\rho}|^2}{2m^2} k^2 d\Omega_k, \qquad E_q(k) = \int \frac{\hbar^2}{2m^2}\left|\widehat{(\boldsymbol{\nabla}\sqrt{\rho})}\right|^2 k^2 d\Omega_k, \tag{4}$$

where the hat denotes the Fourier transform, and Ω_k is the solid angle in Fourier space.

The GPE was evolved in time using a fourth-order Runge-Kutta method, and a pseudospectral method to compute spatial derivatives and nonlinear terms [3]. Time steps were chosen to satisfy the Courant–Friedrichs–Lewy condition, and resulted in $\Delta t = 10^{-3}$ in dimensionles units in simulations with $N_x = N_y = 256$ grid points, and in $\Delta t = 5\times10^{-4}$ in simulations with $N_x = N_y = 512$ grid points. With these choices, total energy is conserved in all simulations up to the sixth significant digit at $t = 10$.

PREPARATION OF THE INITIAL CONDITIONS

An initial random two-dimensional (2D) flow with a three-dimensional (3D) perturbation is constructed using a Clebsch representation of the incompressible velocity field $\boldsymbol{u} = \lambda\boldsymbol{\nabla}\mu - \boldsymbol{\nabla}\phi$, [1], where the Clebsch potentials are a

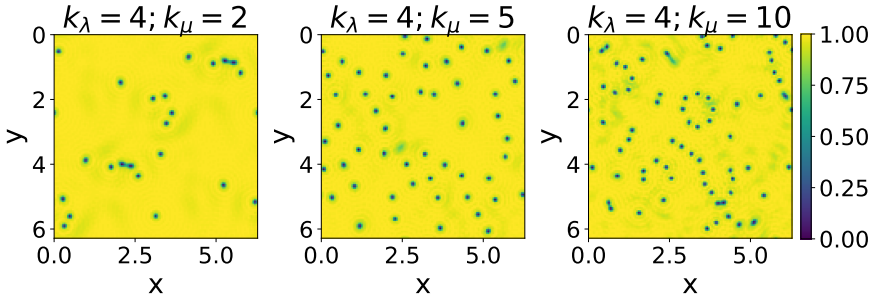

FIG. 1. Slices of the mass density in an xy plane for initial conditions with different values of k_λ and k_μ and with $A_z = 0$. Dark regions correspond to vortex cores. Note the random spatial distribution of vortices, and the change in their number and mean separation as k_μ is varied (similar results are obtained when k_λ is changed).

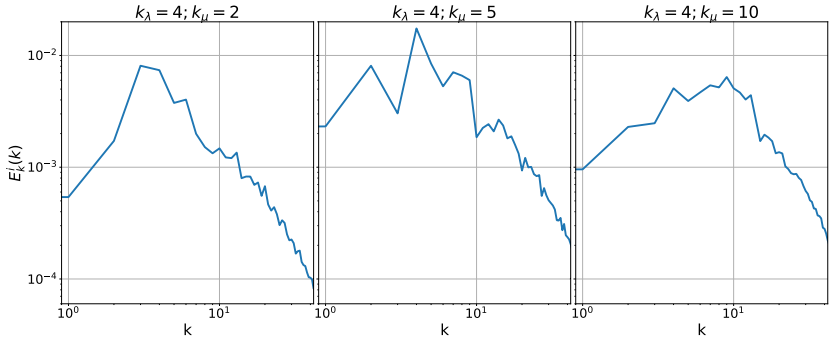

FIG. 2. Incompressible kinetic energy spectrum for the initial conditions in Fig. 1. The wavenumber corresponding to the maximum of the kinetic energy spectral density changes with k_λ and k_μ.

superposition of modes

$$\lambda = \frac{1}{2k_\lambda}\sum_{k_i=1}^{2k_\lambda}\cos\left\{x\left[k_\lambda\cos\left(\frac{\pi k_i}{2k_\lambda}\right)\right] + y\left[k_\lambda\sin\left(\frac{\pi k_i}{2k_\lambda}\right)\right] + \phi_{k_i}\right\}\times\left\{1 + A_z\cos\left(\frac{2\pi z}{L_z} + \varphi_{k_i}\right)\right\}, \tag{5}$$

$$\mu = \frac{1}{2k_\mu}\sum_{k_j=1}^{2k_\mu}\cos\left\{x\left[k_\mu\cos\left(\frac{\pi k_j}{2k_\mu}\right)\right] + y\left[k_\mu\sin\left(\frac{\pi k_j}{2k_\mu}\right)\right]\right\}, \tag{6}$$

where ϕ_{k_i} and φ_{k_i} are random phases, the brackets $[\,.\,]$ indicate the integer part of the argument (to satisfy periodicity of each mode), and k_z is the wavenumber of the perturbation in the z direction. The Clebsch potential ϕ is determined by the condition $\boldsymbol{\nabla}\cdot\boldsymbol{u} = 0$. The parameters k_λ and k_μ control the initial correlation length of the field, and A_z controls the amplitude of the 3D perturbation. The initial conditions are designed to generate a disordered flow with quantized vortices that have a dominant 2D component, a 3D perturbation (when $A_z \neq 0$), and a correlation length at intermediate scales (or wavenumbers) such as both direct or inverse cascades can develop. As described in [1, 2], with these potentials an associated initial wavefunction $\psi(x, y, z)$ can be constructed as the product of wavefunctions $\psi_e(\lambda(x, y, z), \mu(x, y, z))$ where the ψ_e have zeros at the zeros of the Clebsch potentials (and thus quantized vortices in the corresponding x, y, and z coordinates). To reduce the contribution of compressible modes and the initial emission of phonons, before solving the GPE these initial conditions are integrated to convergence using the advective real Ginzburg-Landau equation [1, 2], which is the imaginary-time propagation of the GPE Galilean transformed to preserve the velocity field $\boldsymbol{u}$. The final result is a wavefunction compatible with the flow $\boldsymbol{u}$ and with minimal sound emission, and which is used as the actual initial condition of the GPE.

As examples of the resulting initial conditions, Fig. 1 shows slices in an xy plane of the mass density using 128^3 spatial grid points, for $k_\lambda = 4$ and different values of k_μ (and with $A_z = 0$, and thus 2D). Points with zero density are defects that correspond to quantized vortices. As the number of excited modes increases (i.e., as k_μ increases), more vortices are generated, and the average distance between them decreases. Figure 2 shows the spectrum of the incompressible kinetic energy for each of these initial conditions, and it can be seen that the maximum of the spectrum

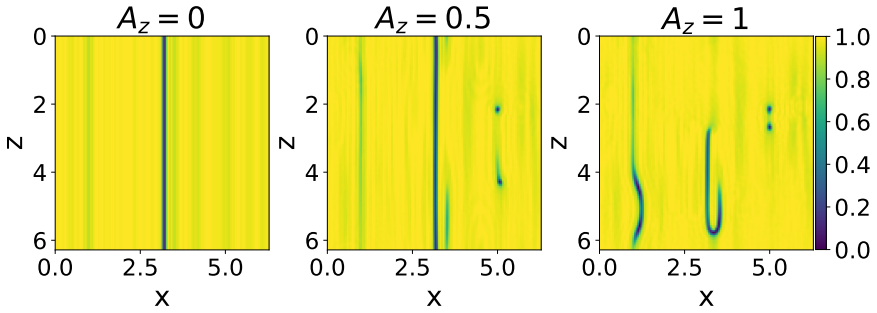

FIG. 3. Slices of the mass density in an xz plane for initial conditions with different values of A_z. Dark regions correspond to vortex cores. The configuration is independent of z for $A_z = 0$, while the vortex cores become more deformed in the vertical direction as A_z is increased.

takes place at a wavenumber that increases with k_μ (i.e., the initial correlation of the flow changes as this quantity is varied) in accordance with the relation $k_\ell \sim \sqrt{M k_0 k_\xi}$ with M the Mach number and $k_\xi \sim 1/\xi$, both of them fixed values, and $k_\ell \sim 1/\ell$ the wave number associated with the intervortex distance ℓ [1]. Similar results are obtained when k_λ is varied. To consider an initial flow with scale separation such that both direct and inverse energy cascades can develop, all simulations in this study are done with $k_\lambda = 4$ and $k_\mu = 10$, such that the initial energy peaks at $k_0 \approx 10$.

The effect of varying A_z is illustrated in Fig. 3, which shows slices in the xz plane of the mass density for initial conditions with fixed k_λ and k_μ, and with different values of A_z. For $A_z = 0$ vortices are parallel and straight in the z direction, and thus generate a purely 2D flow. As A_z increases the vortices curve until in some cases they can even close on themselves forming rings, generating an initially 3D flow. Videos of these initial conditions in cubic boxes and in thin domains, as well as of their time evolution under the GPE, can be seen as supplemental material.

For the study of the transition in cubic boxes, we considered in simulations with $N_x \times N_y \times N_z = 512^3$ grid points values of $A_z = 1$, 0.4, 0.1, 5×10^{-2}, 4×10^{-2}, 3×10^{-2}, 10^{-2}, 8×10^{-3}, 6×10^{-3}, 10^{-3}, 8×10^{-4}, 7×10^{-4}, 6×10^{-4}, 3×10^{-4}, 10^{-5}, and 0 (even more values of A_z, in the same range, were considered in the simulations with $N_x \times N_y \times N_z = 256^3$, for a total of 33 simulations at this resolution). In the thin domain case, the 3D perturbation was fixed at $A_z = 0.1$, and the aspect ratio was varied to take values $\gamma = 1$, 1/2, 1/4, 1/8, 1/10, 1/12.5, 1/16, 1/20, 1/32, and 1/64. As a result, a total of 59 simulations with different parameters was considered for the analysis.

ENERGY FLUXES

Under the GPE, the dynamics of the system conserves the total energy

$$\frac{dE}{dt} = 0, \tag{7}$$

which as a result implies that a detailed balance equation can be written in spectral space as

$$\frac{dE}{dt}(k) = T(k), \tag{8}$$

where $T(k)$ is the transfer function [4–6]. In other words, the change of energy at any given wavenumber must correspond to a transfer of this energy to or from this wavenumber to all other wavenumbers. By integrating this equation up to some wavenumber, an energy flux can be defined as

$$\Pi(k) = -\int_0^k T(k')dk' = -\frac{d}{dt}\int_0^k E(k')dk' = -\frac{dE^<(k)}{dt}. \tag{9}$$

Using the decomposition of the energy in Eq. (2) and the Helmholtz decomposition, this flux can be further decomposed as

$$\Pi(k) = \Pi_k^i(k) + \Pi_k^c(k) + \Pi_{\rm int}(k) + \Pi_q(k), \tag{10}$$

where each component of the flux corresponds to the different energy components. We verified that similar results are obtained when the total energy flux $\Pi(k)$ is used to measure the direction of the cascades, and when the flux of incompressible kinetic energy $\Pi^i_k(k)$ is considered instead.

ESTIMATION OF VORTEX LENGTH

In a similar fashion as with the energy, one can define an incompressible momentum power spectrum. The high wavenumber components of this spectrum can be approximated as the sum of the momenta of all the vortices present in the flow, counted individually. This provides an easy way to estimate the total line length of the vortices in the flow. The method is detailed in references [1, 7].

MOVIES

The movies provided as supplemental material span the entire time evolution of the flow (from $t = 0$ to 10). The 3D renderings of quantized vortices in these movies provide examples of the behavior above and below the critical parameter A_z^c or γ^c (or, in other words, 2D-like and 3D-like behavior), and correspond to the following cases:

- Files side_0003.mp4 and side_4.mp4 are two examples of vortex evolution in the $3D$ cubic domain (at 512^3 resolution), respectively with $A_z = 0.0003$ ($A_z < A_z^c$) and with $A_z = 0.4$ ($A_z > A_z^c$). In the case with $A_z < A_z^c$, note the system remains quasi-2D for a long time, until eventually 3D perturbations grow and dominate the dynamics.

- Files aniso_125.mp4 and aniso_03125.mp4 are two examples of vortex evolution in the thin domain, one with $\gamma = 0.125$ ($\gamma > \gamma^c$) and the other with $\gamma = 0.03125$ ($\gamma < \gamma^c$). In the case with $\gamma < \gamma^c$ the flow remains quasi-2D at all times, showing no vortex reconnection and spatial aggregation of quantized vortices.

[1] C. Nore, M. Abid, and M. Brachet, Physics of Fluids **9**, 2644 (1997).
[2] P. Clark di Leoni, P. D. Mininni, and M. E. Brachet, Physical Review A **95**, 1 (2017).
[3] P. D. Mininni, D. Rosenberg, R. Reddy, and A. Pouquet, Parallel Computing **37**, 316 (2011).
[4] R. Kraichnan and D. Montgomery, Reports on Progress in Physics **43**, 547 (1980).
[5] P. D. Mininni and A. Pouquet, Physical Review E **87**, 1 (2013).
[6] A. Alexakis and L. Biferale, Physics Reports **767-769**, 1 (2018).
[7] V. Shukla, P. D. Mininni, G. Krstulovic, P. Clark di Leoni, and M. E. Brachet, Phys. Rev. A **99**, 043605 (2019).